


2020

Synthesis and Characterization of Tripodal-Imidazolium and Pyridazine Ruthenium Complexes and Their Associated Ligands

Jacqueline L. Kowalke
University of Kentucky, jlkowalke@outlook.com

Follow this and additional works at: <https://uknowledge.uky.edu/honprog>

 Part of the [Life Sciences Commons](#), and the [Medicine and Health Sciences Commons](#)

[Right click to open a feedback form in a new tab to let us know how this document benefits you.](#)

Recommended Citation

Kowalke, Jacqueline L., "Synthesis and Characterization of Tripodal-Imidazolium and Pyridazine Ruthenium Complexes and Their Associated Ligands" (2020). *Lewis Honors College Capstone Collection*. 45.
<https://uknowledge.uky.edu/honprog/45>

This Article is brought to you for free and open access by the Lewis Honors College at UKnowledge. It has been accepted for inclusion in Lewis Honors College Capstone Collection by an authorized administrator of UKnowledge. For more information, please contact UKnowledge@lsv.uky.edu.

Synthesis and Characterization of Tripodal-Imidazolium and Pyridazine Ruthenium Complexes and Their Associated Ligands.

Jacqueline L. Kowalke, John P. Selegue

University of Kentucky

ABSTRACT: Photochemical therapy (PCT) is a relatively new treatment for cancer. PCT, unlike photodynamic therapy (PDT), does not require oxygen though it may be one of the mechanisms that the photosensitizer uses to destroy cancerous cells. Ruthenium complexes have recently entered clinical trials for the treatment of cancer. TLD1433, a ruthenium coordination complex, has entered phase II clinical trials for the treatment of non-muscular invasive bladder cancer. In this compound, the ligands are coordinated via nitrogen bonds, but in this paper, carbon-coordinated complexes are explored. Coordination of N-heterocyclic carbene (NHC) ligands to ruthenium is suspected to provide a different type of coordination complex in PCT. Tripodal and pyridazine NHC ligands were synthesized in this paper, with the tripodal ligand being more successfully produced.

INTRODUCTION

Development of photoactive drugs is a relatively new approach in chemotherapy. Current common chemotherapies fall short because of their general cytotoxicity to healthy cells as well as cancer cells. By controlling the location of the activated drug with light, the use of activated drugs gives hope to treat cancer patients without causing the burden of additional damage to healthy tissue. The use of light, oxygen, and drugs that act as photosensitizers is known as photodynamic therapy (PDT).^{1,2} PDT has been applied in the treatment of many cancers, including lung, esophagus, and skin.³ These are cancers easily accessible from the outside and easily exposed to light. In making these compounds, there are many desirable qualities: inert in the dark, active in the visible light region, and easily synthesized.³

There are two types of photoprocesses in PDT.⁴ Type I photoprocesses involve the electron transfer from photosensitizer to ground-state oxygen ($^3\text{O}_2$) to produce superoxide (O_2^-) and hydroperoxyl radicals (HO_2^\cdot).⁴ These both cause biomolecule degradation and tissue damage or destruction in the body.⁴ Type II PDT agents generate singlet oxygen via the energy transfer from the triplet state of the photosensitizer to the ground state of oxygen. Type II PDT agents target unsaturated lipids, amino acid side chains, and nitrogenous bases.⁴ PDT can also target cancer cells by binding molecules that attach to surface receptors that are extremely common on cancer cells.⁴ These molecules that photosensitizers can bind include antibodies, peptides, proteins, epidermal growth factors, insulin, low-density lipoproteins (LDL), carbohydrates, somatostatin, folic acid, and more.⁴ There has also been intracellular targeting of mitochondria to promote apoptosis via the intracellular apoptotic pathway.⁴

Ideally, photosensitizers should have the following qualities according to Monro, et al.: (1) effective singlet oxygen generation even in hypoxic (low oxygen) environments, (2) large molar extinction coefficient for a wavelength specialized for a type of cancer, (3) specificity for tumor cells, (4) rapid clearance from the body, (5) inactivity in the dark (non-toxicity), (6) chemical stability, (7) availability for injection into the body (most predominantly by dissolution in aqueous solution), (8) easily synthesized and purified.⁴ Many tumors survive in hypoxic environments or create hypoxic environments due to their density and affinity for glycolysis as a source of

energy. This makes them difficult to treat with current PDT agents that rely on oxygen.

Metal coordination complexes are advantageous for many reasons: range of oxidation states, coordination numbers, variable geometries, multiple electronic transitions, lower-energy and longer-lived triplet states, and oxygen-independent mechanisms of cell death.⁴ Low-energy triplet states are important, as the wavelengths of light used to excite the molecules are limited to the energy required to sensitize singlet oxygen (94.5 kJ).⁴ The many electronic transitions possible for transition metal complexes are ligand-to-metal charge transfer (LMCT), intraligand charge transfer (IL), metal-centered charge transfer (MC), and metal-to-ligand charge transfer (MLCT).⁴ MLCT and IL are useful energy transitions in providing energy to convert ground-state oxygen to singlet oxygen. Availability of oxygen-independent mechanisms create the possibility of treating dense and hypoxic tumors. Coordination complexes can attack cancer cells via ligand dissociation independent of oxygen. Specific geometries are required to make an organometallic compound light sensitive.¹ Compounds with distorted octahedral geometry dissociate from their ligands when exposed to light.¹

Current transition metal therapies include platinum amine complexes. Cisplatin (*cis*-diamminedichloroplatinum(II)) intercalates into DNA and causes the cell to have difficulty in any processes involving DNA. Nearly 50% of all cancer treatments are platinum-based.⁴ Despite their relative effectiveness for certain cancers such as prostate cancer, they have many dangerous side effects. Platinum-based drugs are renally toxic, myelosuppressive, neurotoxic, and ototoxic. Other side effects include nausea, vomiting, hair loss, pain, weakness, anemia, and anaphylactic-like reactions. Platinum therapeutics also have issues with degradation before they reach the target DNA and intrinsic or acquired resistance by cancer cells. One of the most common methods of resistance by cancer cells to cisplatin is decreased accumulation or increased efflux by copper-transporter 1 and ATPases 7A/7B, respectively. Glutathione also binds and deactivates cisplatin.³ Therefore, there are many qualities of platinum drugs that cause them to be harsh cancer treatments.

Platinum(II) only has the ability to bind to four ligands at a time. Ruthenium, as is used in these experiments, is able to coordinate to six ligands at one time. This makes it a more flexible metal to use as a metal center. It is also in the same group as iron; this makes it more likely to be taken up by cells.⁵ Furthermore, there is the possibility of replacing the central ruthenium with iron after the complex has been created. This would make the drug less expensive to produce and more environmentally friendly. Ruthenium also has the advantage over platinum by being reductively activated in cells.⁶ In addition, ruthenium compounds are active against some cisplatin-resistant cell lines and have fewer side effects as they are more selective for cancer cells.⁶

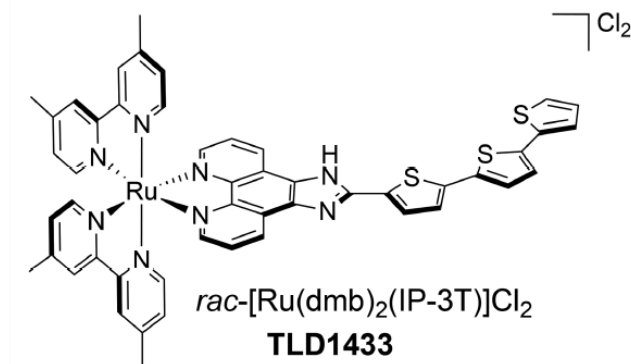


Figure 1. Structure of TLD1433. This figure has been borrowed from the literature.⁴

The ruthenium complex TLD1433 (Figure 1) has reached phase II clinical trials for non-muscular invasive bladder cancer.⁴ The complex participates in many electronic transitions. Its excitation by light brings it to the ¹MLCT state that then relaxes to a ³IL state that creates a long-lived (~100s of microseconds) excited-state equilibrium with a ³IL state located on the thiophene conjugated ligand. This long-lived excited state can very efficiently generate ¹O₂ from the ³IL state.⁴ In addition, this complex can participate in oxygen-independent mechanisms by electron transfer from the triplet intraligand charge transfer (³ILCT) state.⁴

Three other ruthenium compounds have been tested in clinical trials: NAMI-A, KP1019, and KP1339 (Figure 2). Unfortunately, NAMI-A and KP1019 did not make it past phase II clinical trials.⁶ KP1339 is still under consideration in clinical trials.⁶

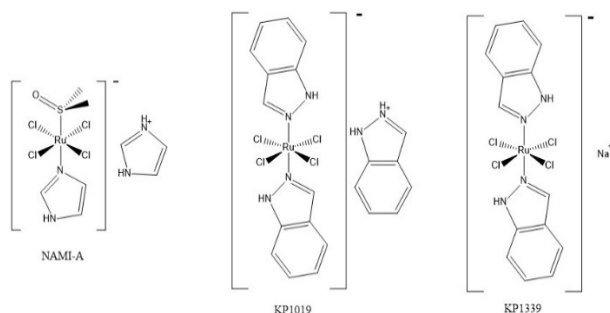


Figure 2. Ruthenium complexes that have been through clinical trials.⁶

All the ruthenium compounds shown above include at least one nitrogen ligand. In my experiments, one or more ligands are coordinated via the carbon atom of a N-heterocyclic carbene (NHC). NHCs were chosen as ligands due to their strong σ donation, ability to make very stable compounds, and drastic effects on electronic properties, such as excited-state lifetimes, which are important for PDT. The resonance structures of the carbene used in my experiments are shown in figure 3. NHCs also can engage in π -donation or π -backbonding.⁷

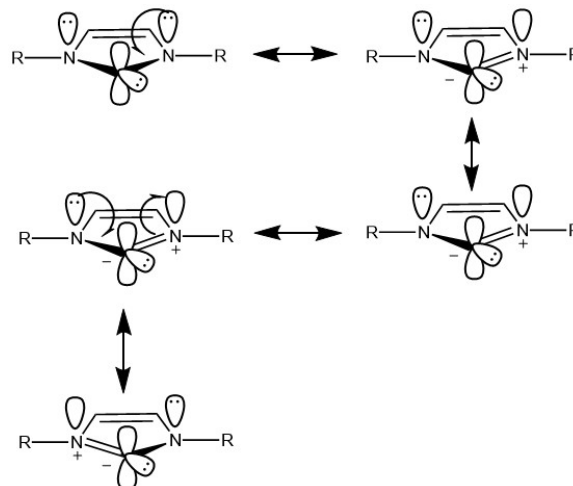


Figure 3. Electron push diagrams illustrating resonance around the carbene.

When the NHCs bind to a metal atom, they strongly donate to the metal, for example, pushing a *trans*-chloride away from the central metal and making it more easily replaced (Figure 4).

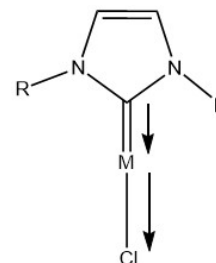
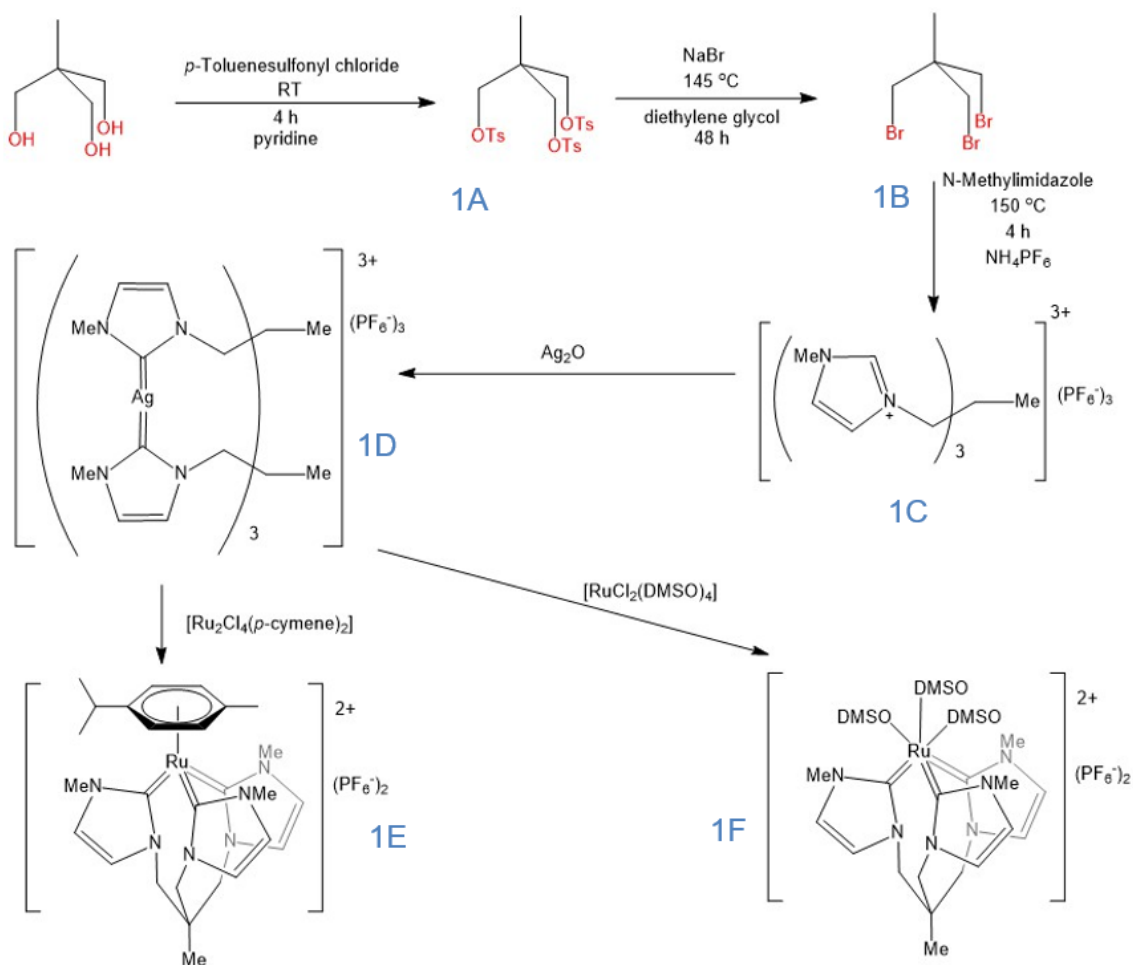


Figure 4. Lengthening of the M-Cl bond is emphasized to show the strong donation effect from the carbene to the metal and the weakening of the Cl-M bond.

In this paper, the synthesis and characterization of imidazolium and pyridazolium ligands and their attempted coordination will be described.

SYNTHESIS

1,1,1-Tris[(*p*-toluenesulfonato)methyl]ethane (1A). 1,1,1-Tris(hydroxymethyl)ethane (33.68 g) was dissolved in pyridine (100 mL) at 0 °C. *p*-Toluenesulfonyl chloride (164.0 g) was dissolved in pyridine (100 mL) and slowly added to the mixture. The



Scheme 1. Reaction scheme of the tripod complexes stirred in the dark under nitrogen for 48 h. The solution was filtered through Celite and the filtrate was brown. The filtrate was cooled in dry ice and DI water was added. No precipitate formed.

flask was removed from the ice bath and set to stir at room temperature for 4 h. The slurry was mixed with HCl (200 mL) and methanol (100 mL). A gummy solid formed in the flask. Methanol was poured over the gummy mass and stirred until white solid precipitated. The white solid was vacuum dried overnight and then oven dried overnight. 132.22 g of product collected.⁸⁻¹¹

1,1,1-Tris(bromomethyl)ethane (1B). **1A** (46.03 g) and NaBr (83.02 g) were mixed in diethylene glycol (250 mL). The reaction mixture was heated to 145 °C and stirred by an overhead stirrer for 48 h. The solution was washed with DI H₂O (250 mL) and three times with ethyl ether (50 mL). The organic phase was dried with MgSO₄, filtered, and evaporated to dryness. 15.56 g of brown oil was collected as product.^{12, 13}

1,1,1-Tris[(n-methylimidazole)methyl]ethane, [H₃TIME^{Me}](PF₆)₃ (1C). **1B** (1.02 g) was added to n-methylimidazole (2 mL) and heated to 150 °C. The reaction mixture was stirred for 18 h under nitrogen. A peanut-butter-like precipitate formed in the bottom. The precipitate was washed with ethanol and white precipitate formed. The white solid was dissolved in methanol and NH₄PF₆ (1.95 g) was added. White powder precipitated (121 mg).¹²

[(TIME^{Me})₂Ag₃](PF₆)₃ (1D) Trial 1. [H₃TIME^{Me}](PF₆)₃ (200 mg) was added to a solution of DMSO (20 mL) and Ag₂O (97 mg). The reaction was stirred in the dark under nitrogen for 12 h at 75 °C. A white-yellow precipitate was obtained (199 mg) and stored in the dark.¹²

[(TIME^{Me})₂Ag₃](PF₆)₃ (1D) Trial 2. [H₃TIME^{Me}](PF₆)₃ (1.02 g) was added to a solution of DMSO (100 mL) and Ag₂O (496 mg). The reaction was stirred in the dark for 24 h at 75 °C. The slurry was filtered through Celite, but no precipitate collected in frit. DI water was added to filtrate to precipitate solid and washed with ether. No solid precipitated. The solution was vacuum dried and then put in an ice bath to condense, but no solid precipitated. No product was collected.

[(TIME^{Me})₂Ag₃](PF₆)₃ (1D) Trial 3. [H₃TIME^{Me}](PF₆)₃ (1.00 g) was added to a solution of DMSO (100 mL) and Ag₂O (486 mg). The reaction mixture was stirred in the dark under nitrogen for 18 h at 75 °C. It was taken off heat and chilled in an ice bath. The entire solution froze and was allowed to melt. The mixture was very gray. It was put back on heat for 20 h at 100 °C. The solution was filtered through Celite. The filtrate was put in an ice bath and lacked the gray color. After adding equal amounts of water, it was washed five times with ether (25 mL). It was then vacuum dried, and a white powder precipitated (716 mg).

[(TIME^{Me})₂Ag₃](PF₆)₃ (1D) Trial 4. [H₃TIME^{Me}](PF₆)₃ (2.92 g) was added to a solution of Ag₂O (1.44 g) and DMSO (100 mL). The reaction mixture was stirred at 75 °C for 18 h under nitrogen in the dark. The solution was filtered through Celite, and grey solid collected in the frit. The filtrate was brown. Filtrate was chilled in an ice bath for 20 min, and then DI water was added. The solution was stirred in the ice bath for 40 min. It was then poured through a frit,

but nothing collected in the frit. More water was added, and the solution chilled in the ice bath again. No precipitate formed.

[(TIME^{Me})₂Ag₃](PF₆)₃ (1D**) *Trial 5.* [H₃TIME^{Me}](PF₆)₃ (1.0 g) was added to a solution of Ag₂O (1.00 g) and DMSO (100 mL). The reaction mixture was heated to 100 °C and stirred in the dark under nitrogen for 48 h. The solution was filtered through Celite, and the filtrate was brown. The filtrate was cooled in dry ice, and DI water was added. No precipitate formed.**

[(TIME^{Me})₂Ag₃](PF₆)₃ (1D**) *Trial 6.* [H₃TIME^{Me}](PF₆)₃ (200 mg) was added to a solution of Ag₂O (101 mg) and dry DMSO (20 mL) in a Schlenk flask that had been dried in an oven at 120 °C. The reaction mixture was stirred in the dark at 100 °C for 15 h under nitrogen. The solution was filtered through Celite, and the filtrate came out clear. The filtrate was cooled to room temperature, and an equal amount of DI water was added. The mixture chilled in an ice bath in the dark for 2 h. Ether was then added and stirred in the flask. Brown precipitate collected.**

(1E) Trial 1. [Ru₂Cl₄(p-cymene)₂] (54 mg) was added to a mixture of **1D Trial 1** (92 mg) in dichloromethane (30 mL). The reaction mixture was stirred for 20 h at room temperature in the dark. The suspension was filtered through Celite and washed with dichloromethane. Hexanes were added to precipitate the product. A light orange solid was collected after vacuum drying (42 mg). The product was insoluble in chloroform but soluble in acetone. A ¹H NMR was run in acetone.

(1E) Trial 2. [H₃TIME^{Me}](PF₆)₃ (230 mg) was added to a solution of Ag₂O (54 mg) and acetonitrile (10 mL). The reaction mixture was stirred at 60 °C under nitrogen, in the dark, for 5 h. At this point, Ru₂Cl₄(p-cymene)₂ (192 mg) was added to the reaction mixture. After 18 h of stirring in the same conditions, it was cooled to room temperature. The solution was filtered through Celite. The filtrate was red wine-colored, and there was white precipitate on the Celite. NH₄PF₆ (32 mg) was added to the solution and stirred for 20 min. The solution was filtered through Celite, and some white powder filtered out. The filtrate was still red wine-colored. The acetonitrile was removed on the rotary evaporator. The residue was washed with ethanol. Yellow color came out in the ethanol washes. The ethanol was decanted, and the remaining solution dried on the rotary evaporator. The remaining solution was then washed with ether, and some red color was taken off by the ether. The solution was then dried on the rotary evaporator again, and 42 mg of red product remained.¹⁴

(1E) Trial 3. [H₃TIME^{Me}](PF₆)₃ (235 mg) was added to a solution of Ag₂O (52 mg) and acetonitrile (10 mL). The reaction mixture was heated to 60 °C for 48 h. The slurry was brown, and black chunks precipitated. Ru₂Cl₄(p-cymene)₂ (203 mg) was added to the solution, and heating continued for 3 d. The solution, which had turned red, was allowed to cool to room temperature. It was filtered through Celite, and NH₄PF₆ (44 mg) was added to the filtrate. The solution stirred for 20 min and was filtered through Celite. The filtrate was dried on the rotary evaporator and then washed with ethanol (three times with 5 mL). The ethanol turned yellow. The solution was swirled with ether (three times with 5 mL), and the ether

layer was decanted. What remained in the flask was a red viscous oil. The oil was dried on the rotary evaporator, and bubbles formed that hardened. The red solid was able to be scraped out of the flask and dissolved in acetone for ¹H NMR. 308 mg of red product was collected. Dichloromethane was added to the product and turned orange; not all dissolved in the dichloromethane. The red colored residue remained solid. The red solid was soluble in acetone. Crystallization of each part was attempted in acetone/ether and dichloromethane/ether. Small crystals appeared in the dichloromethane/ether set up after a few days. X-ray crystallography was performed by Dr. Parkin.

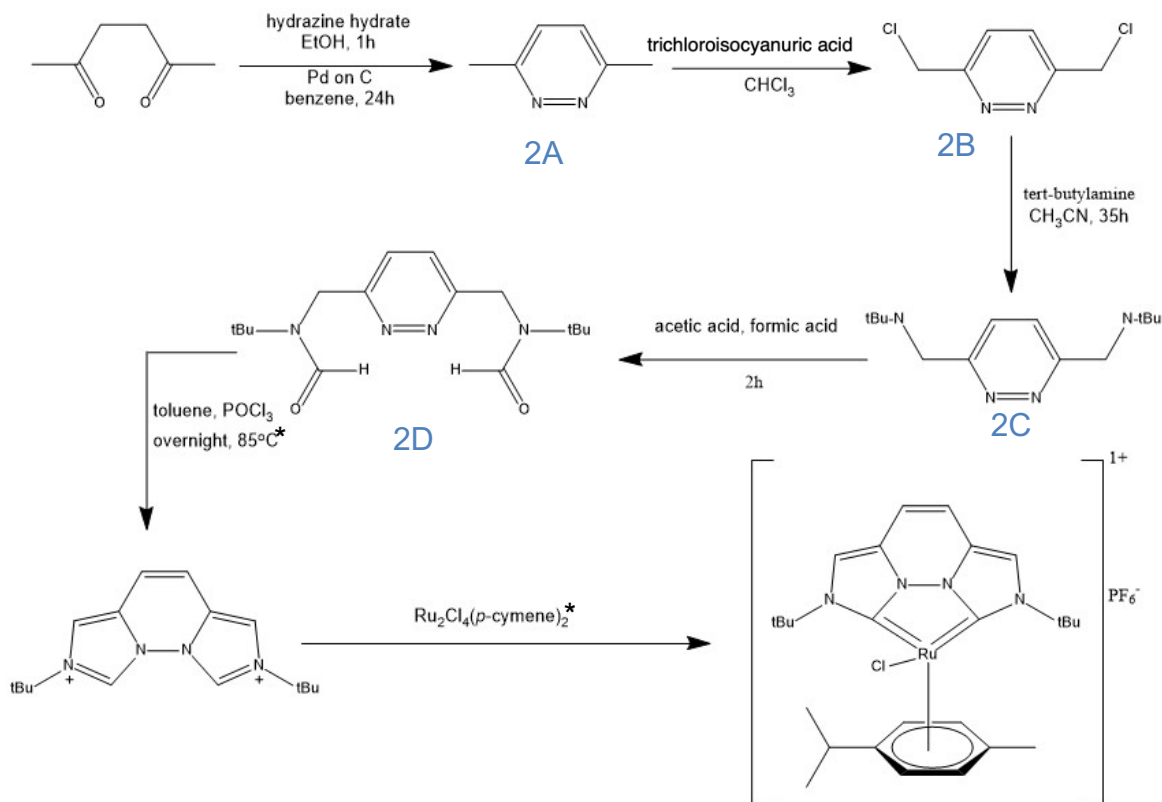
(1E) Trial 4. [H₃TIME^{Me}](PF₆)₃ (270 mg) was added to a solution of Ag₂O (70 mg) and acetonitrile (10 mL). The reaction mixture was heated to 50 °C in the dark under nitrogen for 44 h. After 44 h, Ru₂Cl₄(p-cymene)₂ (214 mg) was added. The mixture stirred at 50 °C for 4 d. The solution was filtered through Celite which removed a white precipitate. The filtrate was placed on the rotary evaporator, and a red oil remained. Crystallization was set up in acetone/ether and DMSO/ether. The acetone/ether crystallization produced small red needle crystals. X-ray crystallography was performed by Dr. Parkin.

(1F) Trial 1. 1D Trial 1 (105 mg) was added to a solution of RuCl₂(DMSO)₄ (86 mg) and dichloromethane/THF (1:1 ratio). The reaction mixture was stirred overnight at 60 °C under nitrogen in the dark. The solution was filtered through a glass frit, and acetone (30 mL) was poured over the collected powder three times. The filtrate was green, and a gray/white powder collected in the frit. Acetone was added to the filtrate to see if product would precipitate – no signs of precipitate. The solid in the frit was washed with acetone; this wash turned gray, but the powder remained gray/white. The grey liquid was rotary evaporated and then evaporated to dryness on the house vacuum. ¹H NMR was taken of the product in acetone as it was insoluble in chloroform.

(1F) Trial 2. 1D Trial 3 (158 mg) was added to a solution of RuCl₂(DMSO)₄ and dichloromethane/THF (1:1 ratio). The reaction mixture was stirred at 60 °C for 58 h in the dark under nitrogen. The solution was filtered through a glass frit. The yellow residue was mixed with acetone, and then the acetone layer was decanted, and the residue vacuum dried. ¹H NMR of the yellow residue was performed in acetone. The solid that collected in the frit was washed with acetone. ¹H NMR in acetone was taken before and after this acetone wash.

(1F) Trial 3. 1D Trial 3 (481 mg) was added to a solution of RuCl₂(DMSO)₄ in dichloromethane/THF (1:1 ratio, 24 mL). The reaction mixture was stirred at 60 °C under nitrogen in the dark for 18 h. The solution turned orange and was poured over a glass frit. The filtrate was mixed with acetone, but no product precipitated. Acetone was poured over the solid in the frit. The solid was vacuum dried and collected as product (466 mg). ¹H NMR was performed in DMSO.

(1F) Trial 4. 1D Trial 3 (103 mg) was added to a solution of RuCl₂(DMSO)₄ (80 mg) and DMSO (5 mL). The reaction mixture



Scheme 2. Reaction scheme of the pyridazine complexes. * indicates that the reaction has not been tested to date.

was heated to 110 °C and stirred in a pressure flask for 24 h in the dark. The solution turned dark yellow. NH_4PF_6 was added. No precipitate. 10 mL of water was added, and still no precipitate formed.

(1F) Trial 5. Product from reaction **1F Trial 3** (191 mg) was assumed to be unreacted **1D Trial 3** and added to a solution of $\text{RuCl}_2(\text{DMSO})_4$ (148 mg) and acetonitrile (50 mL). The reaction mixture was refluxed under nitrogen in the dark for 5 d. During this time, multiple TLCs were performed to assess the progress of the reaction. TLC #1 (silica stationary phase, KNO_3 10% aq./90% MeCN mobile phase) showed movement of the Ru reagent spot, but no movement of the silver reagent or product spot. TLC #2 (silica stationary phase, acetonitrile mobile phase) showed no movement of any of the spots. TLC #3 (silica stationary phase, acetone mobile phase) showed no movement of any of the spots. TLC #4 (silica stationary phase, hexane mobile phase) showed no movement of spots. The initially pale-yellow product that had been removed from the reaction mixture turned pink. After 1 h of heating, the reaction color turned darker yellow. After it was cooled (after 5 d), it was a pink colored solution. It was evaporated to dryness on vacuum line, and the product dried into a dark purple/red solid. The solid was insoluble in acetone, but soluble in DMSO. Crystallization was set up.

(1F) Trial 6. $[\text{H}_3\text{TIME}^{\text{Me}}](\text{PF}_6)_3$ (236 mg) was added to a solution of $\text{RuCl}_2(\text{DMSO})_4$ (34 mg) and 1,2-ethanediol (7 mL) in a pressure flask. The reaction mixture stirred at 180 °C in the dark for 5 h. The solution was filtered through a frit, and white and black powder stayed in the frit. The solids were collected and vacuum dried. They were soluble in DMSO, and ^1H NMR was performed in DMSO.

3,6-Dimethylpyridazine (2A). 2,5-Hexanedione (30 mL, 255 mmol) and hydrazine hydrate (15 mL, 468 mmol) were added to ethanol (250 mL) and heated to reflux for 1 h. The ethanol was

evaporated by rotary evaporation, and a viscous yellow oil was left. Pd on C (1.74 g) and benzene (250 mL) were added to the yellow oil and stirred and heated to reflux (~70 °C) for 18 h. The benzene was evaporated. Then the remaining solution was distilled, and the product came off at a vapor temperature between 60 and 70 °C. The product was a light-yellow oil. ^1H NMR was taken in chloroform. The product was redistilled because the ^1H NMR looked impure. Fraction one of this distillation came off at 40-60 °C. Fraction two came off around 64 °C, and then the vapor temperature dropped. Fraction two was collected as product (5.4 g).¹⁵

3,6-Bis(chloromethyl)pyridazine (2B). 3,6-Dimethylpyridazine (1.042 g) was heated to reflux in chloroform (100 mL). Once reflux was reached, trichloroisocyanuric acid (1.883 g) was added. The reaction mixture turned dark yellow, then pale yellow. After 30 min, the mixture looked like coconut milk. The solution was refluxed for 1 h and then cooled. It was then filtered through Hyflo Celite. The filtrate was washed with NaOH (27 mL) twice, DI H₂O (35 mL) twice, HCl (27 mL) once, and then DI H₂O (35 mL) again. The organic layer was dried with MgSO_4 . The solution was clear and slightly yellow. Chloroform solvent was evaporated off at 0 °C. There was a light brown solid left in the bottom. This solid was purified with flash chromatography (1:4 acetone to pentane). Dark yellow color stayed at the top of the column. 100% yield (1.71 g) assumed and moved on to the next step as product is extremely heat sensitive.¹⁶

3,6-Bis(bromomethyl)pyridazine. 3,6-Dimethylpyridazine (0.5 g) and bromine (1.5 g) was added to acetic acid (35 mL) and heated to 60 °C for 4 h. TLC was performed with 40:60 mL acetone:pentane mobile phase. This TLC was uninformative. The mixture was moved to the rotary evaporator. The product was a brown solid. It was washed with ethyl acetate. Sodium bicarbonate (20 mL saturated) and thionyl chloride (1 g) were added. This mixture was

moved to a separatory funnel, and the ethyl acetate layer was collected. This organic layer was dark brown. It was moved to the house vacuum, and a gum was left as the product. Some part of it was soluble in chloroform, and this part was evaluated by ^1H NMR.

3,6-Bis(*tert*-butylaminomethyl)pyridazine (2C). 3,6-Bis(chloromethyl)pyridazine (1.71 g) and *tert*-butylamine (9.76 mL, 93 mmol) were mixed in acetonitrile (50 mL) for 35 h at room temperature. The solution turned orange and was moved to the fridge. Acetonitrile was evaporated off on the house vacuum line while sitting in an ice bath. A red gummy solid remained (3 g). ^1H NMR done in chloroform.¹⁷

3,6-Bis(*tert*-butylformamidomethyl)pyridazine (2D). 3,6-Bis(*tert*-butylaminomethyl)pyridazine (3 g) was added to formic acid (21 mL, 557 mmol) and stirred for 1.5 h. The mixture turned orange-brown. Acetic acid (21 mL) and distilled water (30 mL) were then added and stirred for 30 min. The solvent was evaporated off at 0 °C. The flask was then filled with nitrogen and placed in the fridge. ^1H NMR was performed in acetonitrile. The ^1H NMR didn't show good differentiation between peaks. Cold acetonitrile was added to the flask and stirred for 10 min and then removed at 0 °C under vacuum. Another ^1H NMR was performed in chloroform. 5.46 g of brown oil was collected.¹⁸

RESULTS

^1H NMR data is displayed in the supporting information included at the end of the paper. TLC data is not included in this paper.

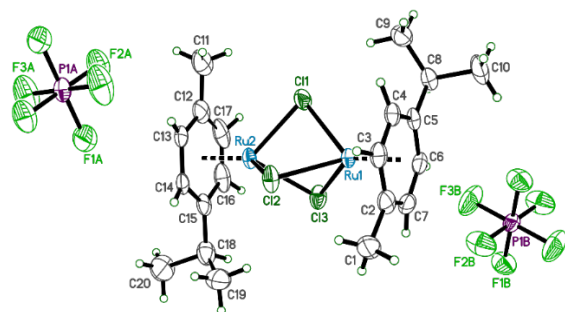


Figure 5. Crystal structure of the product of the red needle crystals produced by reactions **1E Trial 4** and **1E Trial 3**.

X-ray crystallography was performed by Dr. Sean Parkin at the University of Kentucky. The crystals tested were bright red, needle crystals grown as described in the synthesis section. The crystal structure is shown in Fig. 6.

DISCUSSION

The successful synthesis of **1,1,1-tris[(*p*-toluenesulfonato)methyl]ethane** was confirmed by comparison of its ^1H NMR (Fig. 7) with the literature. The ^1H NMR from this experimental spectrum shows peaks at 7.70 (d, 6H), 7.34 (d, 6), 3.77 (s, 6), 2.47 (s, 9), 0.89 ppm (s, 3H); whereas, the literature peaks are at 7.70 (d, 6H), 7.38 (d, 6H), 3.75 (s, 6H), 2.46 (s, 9H), 0.86 (s, 3H).¹⁹ The product was obtained as a white solid in a 79% yield. The next step in this synthesis, **1B**, appears less successful. The ^1H NMR for **1B** did not match previously reported NMR values.²⁰ For example, my product showed peaks and integral values of 3.70 (s, 4H), 3.5 (s, 5H), 1.29 (s, 3H), and 1.25 (s, 1H), which did not agree with previously reported peaks at 3.44 (s, 6H) and 1.22 (s, 3H). All the tosylates seem to be absent

from the product as there are no peaks further down than 4 ppm that could be assigned to the starting material. This could show that there is asymmetry in the compound. This ^1H NMR data suggests the desired product was not formed under these reaction conditions. However, upon the attempted conversion of this sample of **1B** to **1C**, a ^1H NMR spectrum was obtained that closely matched previously reported spectrum for **1C** (Fig. 9). The experimental ^1H NMR peaks were at 9.13 (s, 3H), 7.8 (s, 3H), 7.69 (s, 3H), 4.27 (s, 5H), 3.90 (s, 9H), 0.94 ppm (s, 3H); whereas, the literature reported peaks at 9.12 (s, 3H), 7.82 (s, 3H), 7.68 (s, 3H), 4.26 (s, 6H), 3.89 (s, 9H), 0.93 ppm (s, 3H).¹² This supports that **1B** had successfully been produced but didn't show the same peaks as in the literature. The workup of **1C** may also have been successful in removing any of the contaminant from **1B**. Therefore, the synthesis of **1,1,1-tris[(N-methylimidazole)methyl]ethane (1C)** as presented in this paper is highly reproducible in yielding the desired product. The methods and ^1H NMR presented in this paper show the purest product from the many syntheses.

For the coordination of this ligand to a metal center, two different ruthenium starting materials were chosen based on ease of synthesis, good reactivity, and their presence in the literature.^{21, 22} The synthetic strategy to form ruthenium complexes with **1C** consisted of reacting **1C** with Ag_2O to form an Ag-NHC complex, followed by transmetalation from Ag to Ru(II). The formation of Ru(II) complexes by this method proved to be plagued with problems. Some reactions yielded no precipitate (**1F Trial 4**, **1D Trial 2**, **1D Trial 4**, **1D Trial 5**), and the solution was not evaluated. Some of the problems can be attributed to difficulties forming the Ag-NHC intermediate, $[(\text{TIME}^{\text{Me}})_2\text{Ag}](\text{PF}_6)_3$ (**1D**). One possible cause of this difficulty is likely due to poor quality Ag_2O caused by age and photodecomposition. This suspect Ag_2O was used for **1D Trial 1** as well as a second trial, but failed to yield product, and was replaced with a new bottle. Even with new Ag_2O , the formation of **1D** was unpredictable, and the product was difficult to store. Storage away from light was vital, as **1D** rapidly decomposed from a white solid to a gray solid upon exposure to light, which is common for silver complexes and salts. For these reasons, I began to use a previously reported method where the silver complex was form *in situ* followed by the addition of the Ru(II) starting material.

When reacting $\text{Ru}_2\text{Cl}_4(p\text{-cymene})_2$ with **1D**, **1E Trial 1** showed an ^1H NMR that was extremely similar to the ^1H NMR spectrum of $[(\text{TIME}^{\text{Me}})_2\text{Ag}](\text{PF}_6)_3$ reported by Hu.¹² ^1H NMR of $[(\text{TIME}^{\text{Me}})_2\text{Ag}](\text{PF}_6)_3$ by Hu: 7.55 (s, 3H), 7.49 (s, 3H), 4.44 (s, 3H), 4.20 (s, 3H), 3.90 (s, 9H), 1.24 ppm (s, 3H). This shows that the reaction likely did not proceed past the silver step as there was no evidence of *p*-cymene. For this reason, the product was reused in reaction **1F Trial 5**. The ruthenium product was not crystallized successfully, but ^1H NMR showed that at least there had been a reaction. The peaks appear to be in the right range (between 7 and 8 ppm, around 4 ppm, and 1 ppm as in the silver complex) for the ligand to be attached. Therefore, it is possible that the product may be hiding in that spectrum. The shifts from the silver numbers may be due to the interactions with ruthenium. However, it would need to be purified to be more conclusive. The many peaks may also be due to only a few of the tripod arms being attached. This would create asymmetry and more peak splitting.

In reactions **1F Trial 6** and **1F Trial 2**, the product was clearly not in the ^1H NMR sample. Only solvent and unintended products had been collected. In multiple **1F** and **1E** reactions, I may have collected the wrong product. Early on, some of the reactions produced

precipitate that I then collected as product. However, the actual product may have stayed in solution. This precipitate was most likely AgCl from a reaction between **1D** and chloride ions attached to the metal center. Other salts like this may have precipitated and been collected as product.

A crystal structure collected from reactions **1E Trial 4** and **1E Trial 3** shows that the intended product did not crystallize, but a chloride ion was abstracted from the ruthenium starting material (Fig. 6). It is possible that the intended product did form, but there is no evidence of this as ^1H NMR was not performed. As the $\text{Ru}_2\text{Cl}_2(\text{p-cymene})_2$ is the starting material that self-reacted, the $\text{RuCl}_2(\text{DMSO})_4$ seems to be a good alternative starting material. From the ^1H NMR data (Fig. 12, 14, 15) on the **1F** compounds, it seems likely that the product could be obtained as there were a multitude of peaks in the 7-8 ppm, 4 ppm, and 1 ppm range. The ease of synthesis of the precursor ligand also supports further reactions with $\text{RuCl}_2(\text{DMSO})_4$. Future work with this ligand and ruthenium source could result in complexes with very interesting characteristics of anticancer ruthenium complexes.

The synthesis of **3,6-dimethylpyridazine (2A)** was very easy to perform, and the product could be obtained in high purity by vacuum distillation followed by crystallization on cold storage. The following reaction to produce **3,6-bis(chloromethyl)pyridazine (2B)** was much more difficult. This reaction was run many times with different temperatures and reaction times. Trichloroisocyanuric acid seemed to be the most common chlorination method for this reaction (**2B**), but perhaps it is not the best. The product was difficult to identify in a ^1H NMR or TLC. As it was so heat sensitive, the product was assumed to be produced, and the next step was immediately done as the **3,6-bis(tert-butylaminomethyl)pyridazine** was more stable and, thus, could be more easily tested. The spectrum of **3,6-bis(tert-butylaminomethyl)pyridazine** (Fig. 19) resembles the literature values.¹⁸ ^1H NMR of **3,6-bis(tert-butylaminomethyl)pyridazine** from the literature reported peaks at 7.52 (s, 2H), 4.05 (s, 4H), 1.88 (s, 2H), 1.19 ppm (s, 18H).¹⁸ My spectrum shows peaks at 7.56 (s, 2H), 4.11 (s, 5H), 1.32 (s, 21H), 1.26 (s, 10H), 1.18 ppm (s, 5H). For some peaks, such as 4.05 ppm, this could be due to error in choosing the proper range for the integral. For other peaks, it may be that there is starting material or other contaminants in the same locations that raise the peaks. The issue could also be that the compound only had one tert-butyl-amine group attached, and the other side was a methyl group due to the loss of a chloride. This would lead to asymmetrical peaks.

My products have been overchlorinated and underchlorinated, and it is difficult to determine the perfect reaction conditions. The product is highly heat sensitive, and so the solvent cannot be removed on the rotary evaporator.²³ Thus, the house vacuum with an ice bath was used. However, this evaporation takes a long time; many times I left it overnight to dry. The compound could have self-reacted during this time. It is also frustrating that the product is heat sensitive, yet the reaction is run at reflux. This could cause the product to self-react as soon as it is produced. During one run of this experiment, the reaction mixture heated for 60 min, and a small sample for ^1H NMR was taken every 10 min to monitor reaction completion. Unfortunately, this proved to be unfeasible as the workup for the reaction removed so much of the sample that nothing was left to put in the NMR tube for each of the six samples. The reaction was also difficult to monitor via TLC on silica; though, in theory, this should be possible.

A different method may be a better way to produce the halogenated product. For the reasons discussed above, bromination of **2A** had been attempted but failed under the reaction conditions mentioned in the synthesis section. The ^1H NMR of the bromination, **3,6-bis(bromomethyl)pyridazine**, showed starting material only. Longer reaction times and a higher temperature may be used to push this reaction to completion. Different bromine reactants may also be tested. One that I am particularly interested in testing is NBS; this reagent was not used at the time because it was not readily available in the lab. Perhaps also, if the methyl group can be hydroxylated, the same bromination used in the tripod reactions can be used to brominate the molecule. However, this method may prove more difficult than hypothesized.

The synthesis of **3,6-bis(tert-butylformamidomethyl)pyridazine (2D)** appears to be unsuccessful as the ^1H NMR spectrum is not analogous to the literature (Fig. 20). The experimental ^1H NMR spectrum showed peaks at 7.95 (d, 2H), 7.8 (d, 2H), 7.5 (s, 1H), 7.02 (s, 2H), 5.29 (s, 3H), 4.12 (s, 1H), 2.77 (s, 1H), 1.93 (s, 10H), 7.32 (s, 7H), 1.24 (s, 11H), 1.19 (s, 18H), 1.18 ppm (s, 5H). The literature ^1H NMR for the compound has peaks at 10.22 (s, 2H), 8.35 (s, 2H), 7.46 (s, 2H), 1.79 ppm (s, 18H). The experimental ^1H NMR lacks the 10 ppm peak, which is a big indicator that the product was not present in the reaction I ran. This is likely due to the impurity of the starting material.

CONCLUSION

In conclusion, the reactions illustrated in this paper had varying success. The tripodal ligands were easy to synthesize, but the pyridazine ligands were not. Different methods are needed to coordinate the tripodal ligand to the ruthenium. Different methods are also needed to form the 3,6-Bis(chloromethyl)pyridazine. Future goals for ruthenium complex synthesis are to form a tripod ruthenium complex and find a better method for halogenation of 3,6-dimethylpyridazine.

AUTHOR INFORMATION

Corresponding Author

* Jacqueline Lea Kowalke, jlkowalke@outlook.com

ACKNOWLEDGMENT

I am extremely appreciative of the support and direction given by my professor, Dr. J.P. Selegue. I am also very thankful to Raphael Ryan, without whom I could not have performed my research nor completed this paper. Thanks also go to Dr. Edith Glazer for teaching me about DNA damage, cancer, and its treatments; Dr. Sean Parkin for his skill in crystallography; and Dr. Justin Mobley for teaching me how to use the Bruker NMR machine. I also greatly appreciate the funding provided from UK in the form of the "Bucks4Brains" scholarship that allowed me to perform research over the past two summers.

REFERENCES

1. Howerton, B. S.; Heidary, D. K.; Glazer, E. C., Strained ruthenium complexes are potent light-activated anticancer agents. *J. Am. Chem. Soc.* **2012**, *134*, 8324-8327.
2. Monro, S.; Colón, K. L.; Yin, H.; Roque, J.; Konda, P.; Gujar, S.; Thummel, R. P.; Lilje, L.; Cameron, C. G.; McFarland, S. A., Transition Metal Complexes and Photodynamic Therapy from a Tumor-Centered Approach: Challenges, Opportunities, and Highlights from the Development of TLD1433. *Chem. Rev.* **2019**, *119*, 797-828.

3. Howerton, B. S.; Heidary, D. K.; Glazer, E. C., Strained ruthenium complexes are potent light-activated anticancer agents. *Journal of the American Chemical Society* **2012**, 134 (20), 8324-8327.
4. Monro, S.; Colón, K. L.; Yin, H.; Roque, J.; Konda, P.; Gujar, S.; Thummel, R. P.; Lilje, L.; Cameron, C. G.; McFarland, S. A., Transition Metal Complexes and Photodynamic Therapy from a Tumor-Centered Approach: Challenges, Opportunities, and Highlights from the Development of TLD1433. *Chemical reviews* **2019**, 119 (2), 797-828.
5. Thota, S.; Rodrigues, D. A.; Crans, D. C.; Barreiro, E. J., Ru(II) Compounds: Next-Generation Anticancer Metallotherapeutics? *J. Med. Chem.* **2018**, 61, 5805-5821.
6. Thota, S.; Rodrigues, D. A.; Crans, D. C.; Barreiro, E. J., Ru(II) Compounds: Next-Generation Anticancer Metallotherapeutics? *Journal of medicinal chemistry* **2018**, 61 (14), 5805-5821.
7. Nelson, D. J.; Nolan, S. P., Quantifying and understanding the electronic properties of N-heterocyclic carbenes. *Chem. Soc. Rev.* **2013**, 42, 6723-6753.
8. Hu, X.; Castro-Rodriguez, I.; Olsen, K.; Meyer, K., Group 11 Metal Complexes of N-Heterocyclic Carbene Ligands: Nature of the MetalCarbene Bond. *Organometallics* **2004**, 23, 755-764.
9. Ure, A. D.; Lzaro, I. A.; Cotter, M.; McDonald, A. R., Synthesis and characterisation of a mesocyclic tripodal triamine ligand. *Org. Biomol. Chem.* **2015**, 14, 483-494.
10. Chandrasekaran, V.; Lindhorst, T. K., Sweet switches: azobenzene glycoconjugates synthesized by click chemistry. *ChemComm* **2012**, 48, 7519-7521.
11. Beaufort, L.; Delaude, L.; Noels, A. F., A new tripodal ligand system based on the iminophosphorane functional group. Part 1: Synthesis and characterization. *Tetrahedron* **2007**, 63, 7003-7008.
12. Hu, X.; Castro-Rodriguez, I.; Olsen, K.; Meyer, K., Group 11 Metal Complexes of N-Heterocyclic Carbene Ligands: Nature of the MetalCarbene Bond. *Organometallics* **2004**, 23 (4), 755-764.
13. Petrovski, Ž.; Romão, C. C.; Afonso, C. A. M., Synthesis of Tris(N,N -dimethylthiocarbamoyl)-1,1,1- tris -(methylaminomethyl)ethane and Its Application as Ligand for Pauson–Khand Reaction. *Synth. Commun.* **2008**, 38, 2761-2767.
14. Liu, X.; Chen, W., Synthesis of ruthenium(ii) complexes of tetradentate bis(N -pyridylimidazolylidenyl)methane and their reactivities towards N- donors. *Dalton Trans.* **2011**, 41, 599-608.
15. Wiley, R. H., Poly(DMI-1,2-Diazinediethylene-1,2-Diols). *J. Macromol. Sci.* **1987**, 24, 1183-1190.
16. Wiley, R. H., Poly(DMI-1,2-Diazinediethylene-1,2-Diols). *Journal of Macromolecular Science* **1987**, 24 (10), 1183-1190.
17. Flaig, K. S.; Raible, B.; Mormul, V.; Denninger, N.; Maichle-Mössmer, C.; Kunz, D., Generation of Annelated Dicarbenes and Their Alkali-Metal Chelate Complexes in Solution: Equilibrium between Hetero- and Homoleptic NHC Lithium Complexes. *Organometallics* **2018**, 37, 1291-1303.
18. Flaig, K. S.; Raible, B.; Mormul, V.; Denninger, N.; Maichle-Mössmer, C.; Kunz, D., Generation of Annelated Dicarbenes and Their Alkali-Metal Chelate Complexes in Solution: Equilibrium between Hetero- and Homoleptic NHC Lithium Complexes. *Organometallics* **2018**, 37 (8), 1291-1303.
19. Beaufort, L.; Delaude, L.; Noels, A. F., A new tripodal ligand system based on the iminophosphorane functional group. Part 1: Synthesis and characterization. *Tetrahedron* **2007**, 63 (30), 7003-7008.
20. Petrovski, Ž.; Romão, C. C.; Afonso, C. A. M., Synthesis of Tris(N,N -dimethylthiocarbamoyl)-1,1,1- tris -(methylaminomethyl)ethane and Its Application as Ligand for Pauson–Khand Reaction. *Synthetic communications* **2008**, 38 (16), 2761-2767.
21. Bratsos, I.; Alessio, E., *Ruthenium(II)-Chlorido Complexes of Dimethylsulfoxide*. John Wiley & Sons: 2010; Vol. 35.
22. Bennet, M. A.; Huang, T. N.; Matheson, T. W.; Smith, A. K., *(n6-Hexamethylbenzene)ruthenium Complexes*. John Wiley & Sons: 1982; Vol. 21.
23. Gierz, V.; Maichle-Mössmer, C.; Kunz, D., 1,10-Phenanthroline Analogue Pyridazine-Based N-Heterocyclic Carbene Ligands. *Organometallics* **2012**, 31, 739-747.

SUPPORTING INFORMATION (¹H NMR SPECTRA)

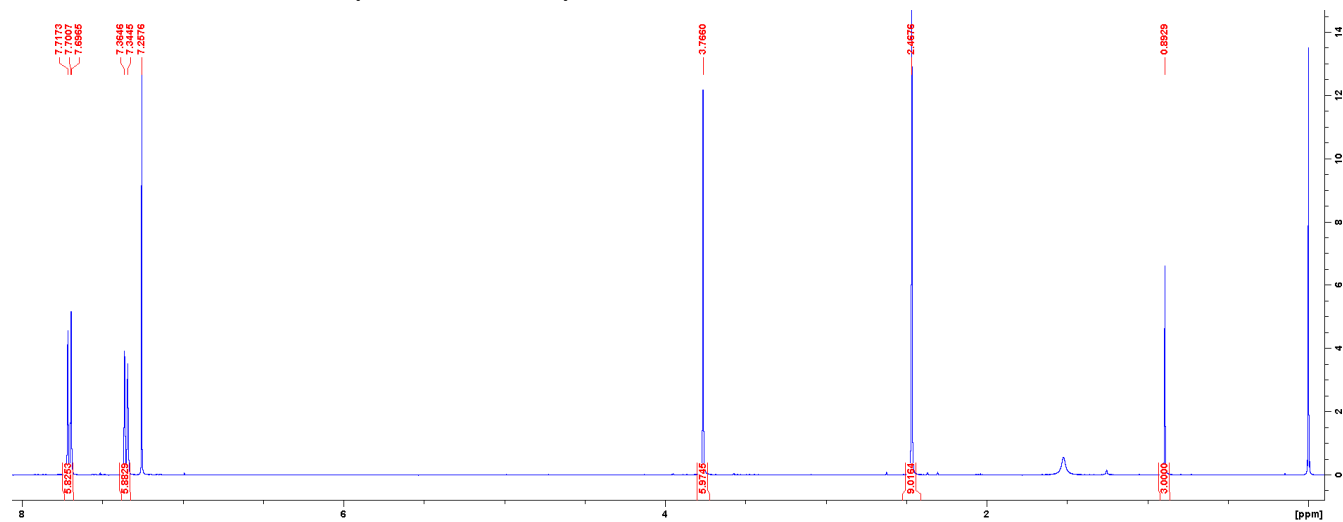


Figure 6. ¹H NMR of 1,1,1-tris[(*p*-toluenesulfonato)methyl]ethane (1A) in chloroform.

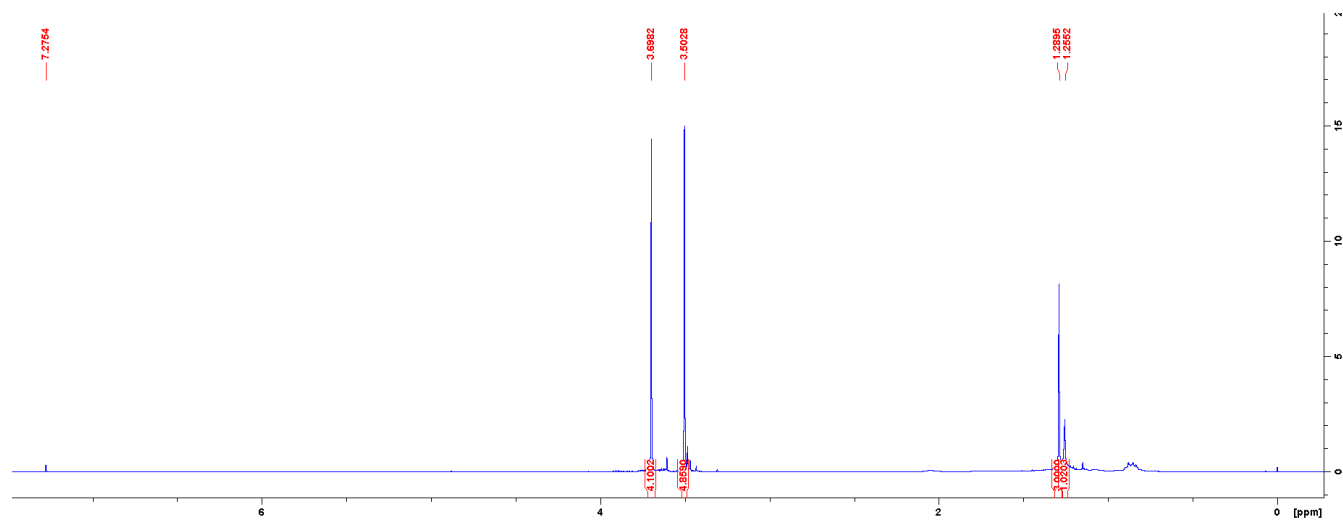


Figure 7. ¹H NMR of 1,1,1-tris(bromomethyl)ethane (1B) in chloroform.

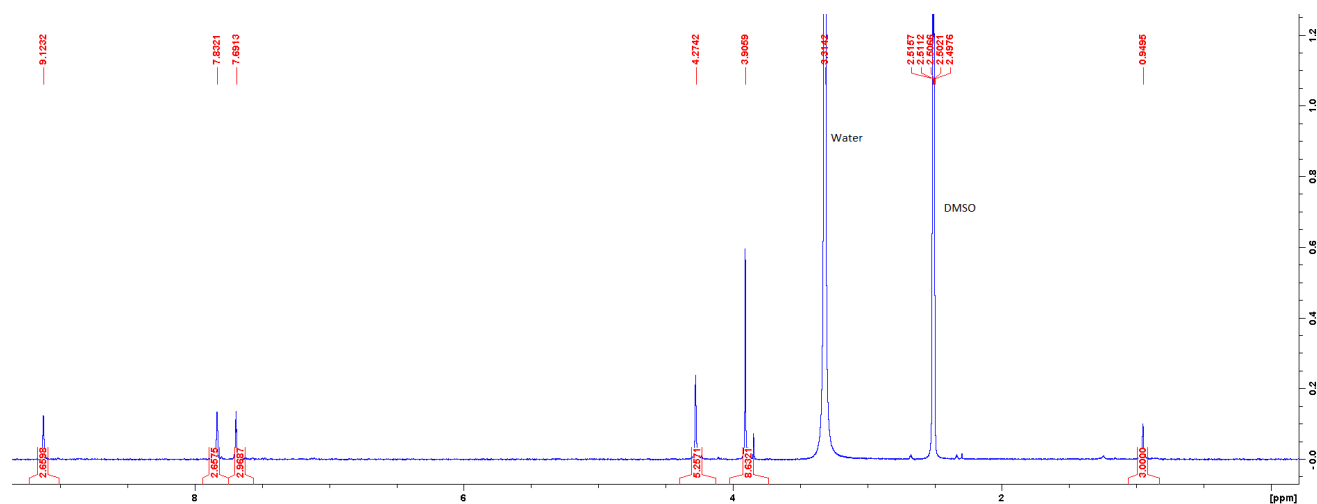
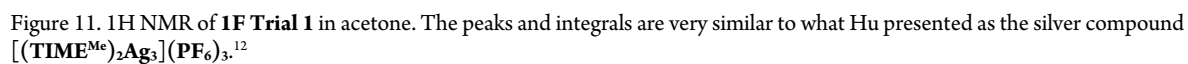
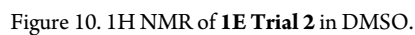
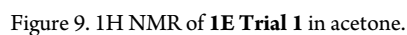


Figure 8. ¹H NMR of 1,1,1-tris[(*n*-methylimidazole)methyl]ethane, [H₃TIME^{Me}](PF₆)₃ (1C) in DMSO.



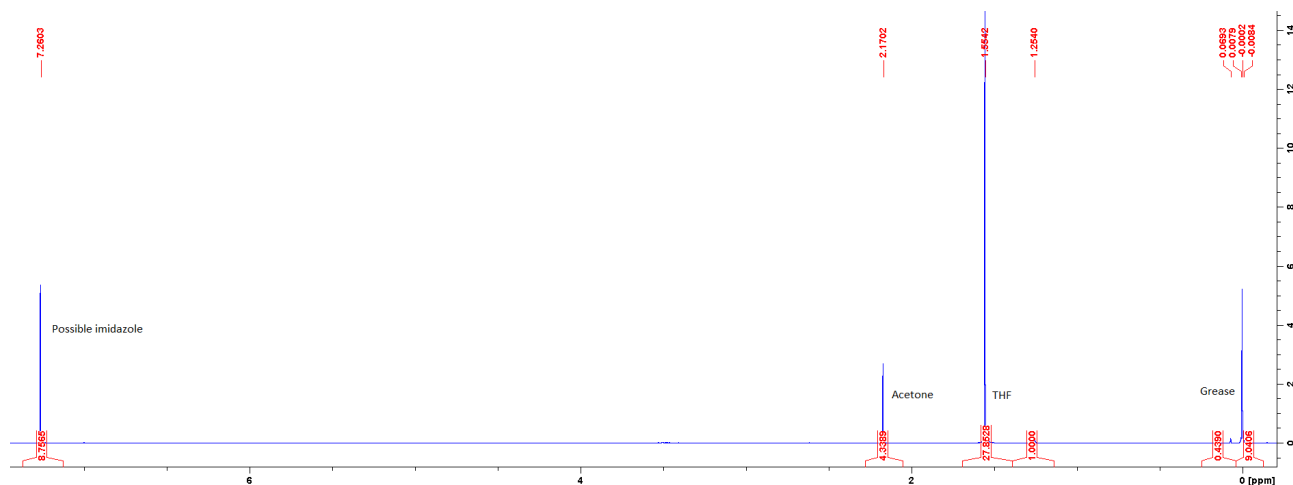


Figure 12. ¹H NMR of **1F Trial 2** yellow filtrate in acetone.

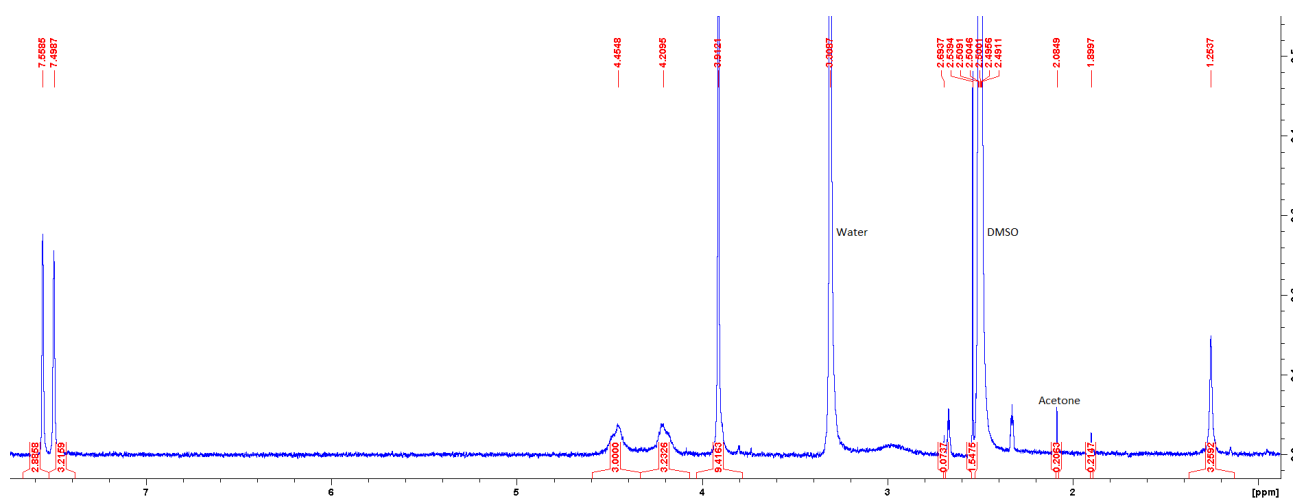


Figure 13. ¹H NMR of **1F Trial 3** solid in DMSO prior to acetone wash. The peaks and integrals are very similar to what Hu presented as the silver compound $[(\text{TIME}^{\text{Me}})_2\text{Ag}_3](\text{PF}_6)_3$.¹²

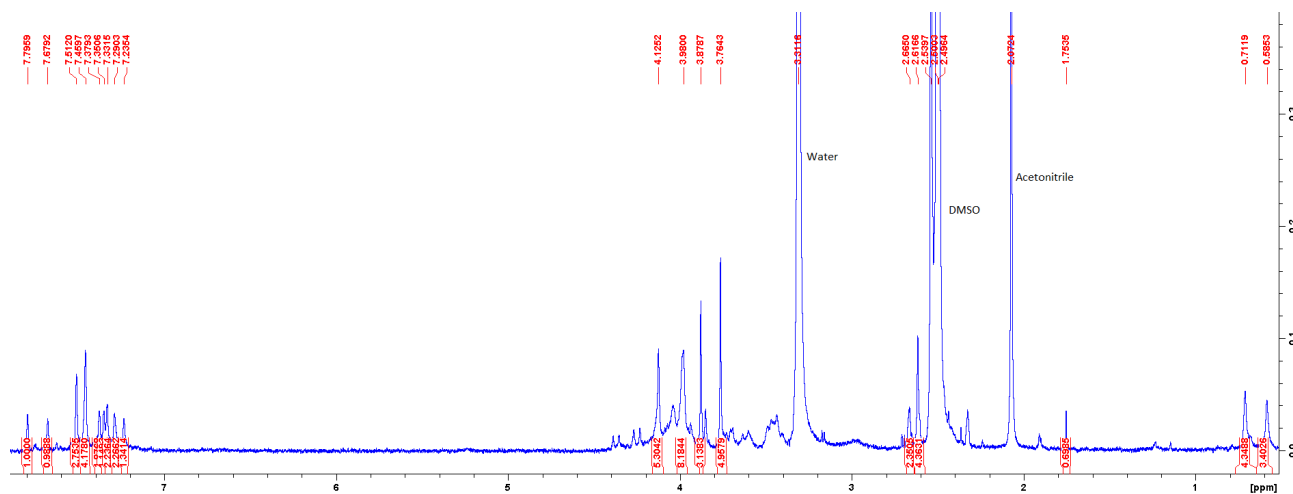


Figure 14. ¹H NMR of **1F Trial 5** in DMSO.

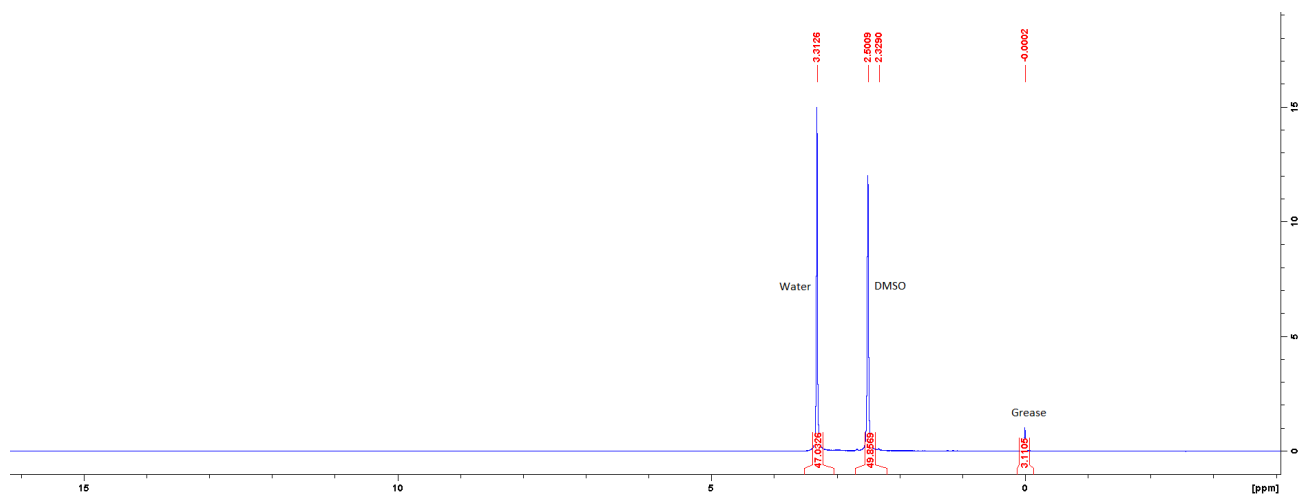


Figure 15. ¹H NMR of solid from **1F Trial 6** in DMSO.

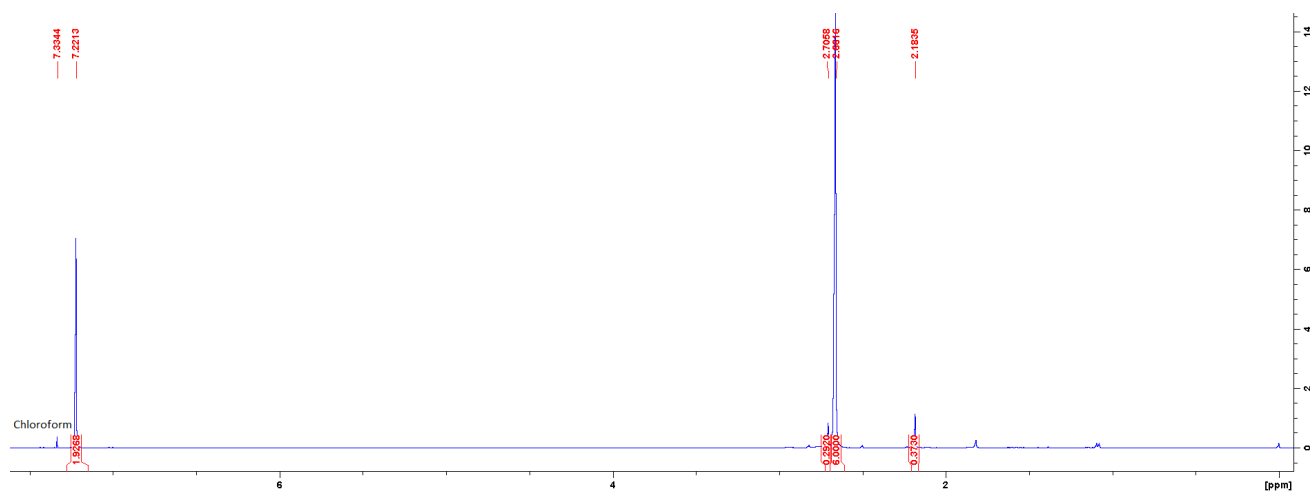


Figure 16. ¹H NMR of **3,6-dimethylpyridazine (2A)** in chloroform.

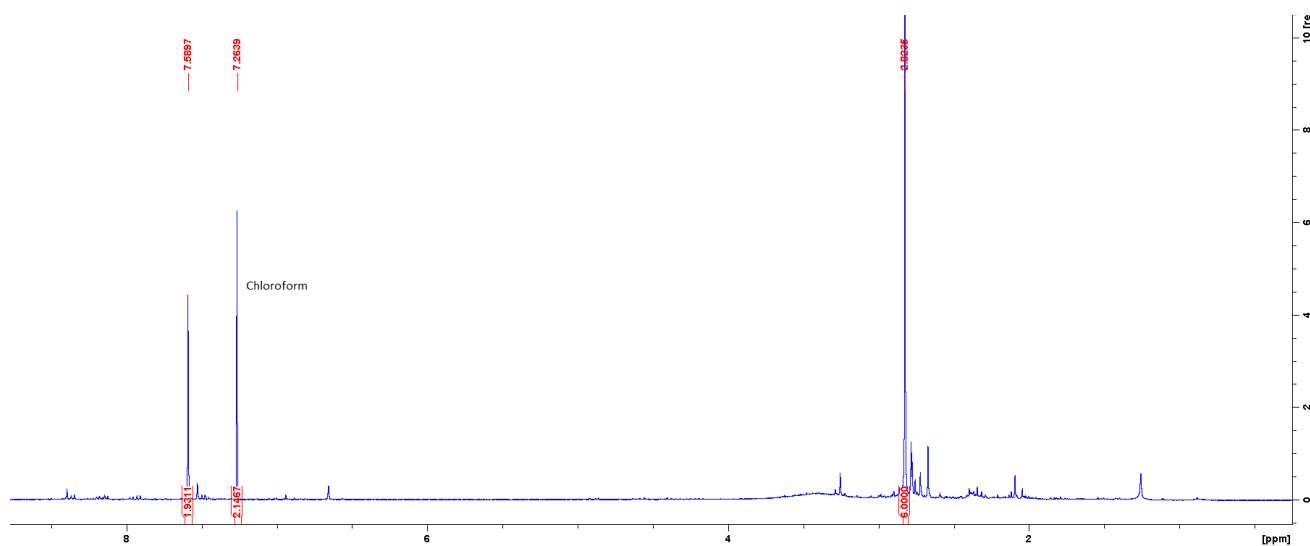


Figure 17. ¹H NMR of **3,6-bis(bromomethyl)pyridazine (2B)** in chloroform.

